



**HAL**  
open science

## Real-time tracking of root hair nucleus morphodynamics using a microfluidic approach

Gaurav Singh, David Pereira, Stéphanie Baudrey, Elise Hoffmann, Michael Ryckelynck, Atef Asnacios, Marie-Edith Chaboute, Marie-edith Chabouté

### ► To cite this version:

Gaurav Singh, David Pereira, Stéphanie Baudrey, Elise Hoffmann, Michael Ryckelynck, et al.. Real-time tracking of root hair nucleus morphodynamics using a microfluidic approach. *Plant Journal*, 2021, 10.1111/tpj.15511 . hal-03357641

**HAL Id: hal-03357641**

**<https://hal.science/hal-03357641>**

Submitted on 28 Sep 2021

**HAL** is a multi-disciplinary open access archive for the deposit and dissemination of scientific research documents, whether they are published or not. The documents may come from teaching and research institutions in France or abroad, or from public or private research centers.

L'archive ouverte pluridisciplinaire **HAL**, est destinée au dépôt et à la diffusion de documents scientifiques de niveau recherche, publiés ou non, émanant des établissements d'enseignement et de recherche français ou étrangers, des laboratoires publics ou privés.

## **Real-time tracking of root hair nucleus morphodynamics using a microfluidic approach**

Gaurav Singh<sup>1a\*</sup>, David Pereira<sup>2a</sup>, Stéphanie Baudrey<sup>3</sup>, Elise Hoffmann<sup>1</sup>, Michael Ryckelynck<sup>3</sup>, Atef Asnacios<sup>2</sup> and Marie-Edith Chabouté<sup>1\*</sup>

<sup>1</sup>Institut de biologie moléculaire des plantes, UPR2357 CNRS, Université de Strasbourg, 67084 Strasbourg France

<sup>2</sup>Laboratoire Matière et Systèmes Complexes, UMR 7057, CNRS and Université de Paris, 75013, Paris, France

<sup>3</sup>Institut de Biologie Moléculaire et Cellulaire du CNRS, Université de Strasbourg, 67084 Strasbourg France

a: These authors contributed equally to this work

\*: Corresponding authors

[marie-edith.chaboute@ibmp-cnrs.unistra.fr](mailto:marie-edith.chaboute@ibmp-cnrs.unistra.fr)

[gaurav.singh@ibmp-cnrs.unistra.fr](mailto:gaurav.singh@ibmp-cnrs.unistra.fr)

**Running title:** A microfluidic device for analysing nuclear morphodynamics.

**Key words:** *Arabidopsis thaliana*, live cell imaging, microfluidics, nucleus, root hair, single cell.

## **Abstract**

Root hairs (RHs) are tubular extensions of root epidermal cells that favour nutrient uptake and microbe interactions. RH shows a fast apical growth, constituting a unique single cell model system to analyse cellular morphodynamics. In this context, live cell imaging using microfluidics recently developed to analyze root development is appealing, but high-resolution imaging is still lacking to study accurate spatiotemporal morphodynamics of organelles. Here, we provide a powerful coverslip based microfluidic device (CMD) which enables us to capture high resolution confocal imaging of *Arabidopsis* RH development with real-time monitoring of nuclear movement and shape changes. To validate the setup, we confirmed the typical RH growth rates and the mean nuclear positioning previously reported with classical methods. Moreover, in order to illustrate the possibilities offered by the CMD, we have compared the real-time variations in the circularity, area, and aspect ratio of nuclei moving in growing and mature RH. Interestingly, we observed higher aspect ratios in the nuclei of mature RH, correlating with higher speeds of nuclear migration. This observation opens the way for further investigations of the effect of mechanical constraints on nuclear shape changes during RH growth and nuclear migration and its role in RH and plant development.

## Introduction

The plant developmental programs were largely investigated at the organ, tissue or whole plant seedling levels, but are also now more and more studied at the single cell level using root hairs, pollen tubes or isolated protoplasts in *Arabidopsis*, soybean and maize (Libault *et al.*, 2010; Qiao *et al.*, 2017; Misra *et al.*, 2019; Ryu *et al.*, 2019; Satterlee *et al.*, 2021; Agudelo *et al.*, 2012). The root hair (RH) is a single differentiated cell from the epidermis that directly interacts with the external environment. RHs are unicellular lateral extensions of root epidermal cells (trichoblast) and display distinct properties concerning cell size, vacuole size and cell surface features (Grierson *et al.*). RH development occurs in three well defined steps: initiation with outgrowth from a trichoblast cell, elongation via tip growth and maturation when the tip stops growing.

At the molecular level, RH growth is a highly regulated process well characterized at the transcriptomic and proteomic levels, notably in soybean (Libault *et al.*, 2010; Brechenmacher *et al.*, 2012). In *Arabidopsis*, RH specific genes and proteins have been identified as important for RH development (Lan *et al.*, 2013; Petricka *et al.*, 2012; Li and Lan, 2015). Indeed, a spatio-temporal gene expression controls RH growth (Shibata *et al.*, 2018; Yi *et al.*, 2010).

At the cellular level, RHs are tubular structures of 10  $\mu\text{m}$  diameter which elongate uniaxially, perpendicular to the main root axis and can reach 1 mm in length (Grierson *et al.*, 2014). RH hair development is tightly controlled by cytoskeleton reorganization and vesicle trafficking controlled by the small Rho GTPases (Krupinski *et al.*, 2016; Kang *et al.*, 2017; Ketelaar *et al.*, 2002; Jones *et al.*, 2002). Tip growth involves trafficking of secretory and endocytic vesicles providing building blocks for cell wall and plasma membrane in the cytoplasmic dense area (Ketelaar *et al.*, 2002; Hepler *et al.*, 2001). A cortical cytoplasm surrounds a vacuole which ensures turgor pressure needed for RH growth (Volgger *et al.*, 2010). RH growth shows variation in its rate with an early growth rate of 0.4  $\mu\text{m}/\text{min}$ , i.e. until RH protrusion reached a size of 20 to 40  $\mu\text{m}$  and a late growth rate of 1 to 2.5  $\mu\text{m}/\text{min}$  (Dolan *et al.*, 1994). During RH growth, the nucleus is at a mean distance of  $77 \pm 15$   $\mu\text{m}$  from the tip (Ketelaar *et al.*, 2002). In mature RH with stopped growth, a basipetal movement of the nucleus occurs randomly with intervals of pausing (Chytilova *et al.*, 2000).

A few studies have shown that nuclear migration in the RH may be associated with various cellular responses against environmental stimuli including symbiosis, plant microbe interaction, nutrient and water uptake as well as response to light (Griffis *et al.*, 2014; Tamura

*et al.*, 2013). During RH growth, the nucleus position and movement appear to be tightly regulated. At least in *Arabidopsis*, they are notably controlled by actin and its associated proteins Myosin XI-i (Ketelaar *et al.*, 2002; Tamura *et al.*, 2013), with the migration direction of RH nuclei being closely related to the perinuclear actin filaments (Zhang *et al.*, 2019).

During RH growth, the nucleus is also described to change its shape (Chytilova *et al.*, 2000). However, no clear correlation between nuclear movement and nuclear shape changes was established. Investigating such a link between nuclear shape changes and nuclear movement during development would be of great interest to understand the role of mechanotransduction in plant growth. Indeed, changes in nuclear shape were recently correlated to the induction of stress responsive and developmental genes during organogenesis (Fal *et al.*, 2021; Landrein *et al.*, 2015) and plant adaptation to their environment (Goswami *et al.*, 2020a; Goswami *et al.*, 2020b).

Thus, in order to study the link between RH growth, nuclear movements and shape changes, we have developed a simple microfluidic platform coupled with high resolution microscopy to monitor in real time nuclear shape and movements during RH development in a controlled and standardized environment. First, to validate this new coverslip based microfluidic device (CMD), we measured various parameters of RH growth well documented in the literature, such as RH velocity and mean nuclear position with respect to RH tip. In addition, as an illustration of the new possibilities offered by the CMD, we report accurate descriptions of nuclear shape changes during RH growth, as well as a significant difference in the nuclear aspect ratio that correlates with a difference in migration speeds for nuclei observed in growing and mature RHs.

## **Results**

### **Experimental setup of the coverslip based microfluidic device (CMD) for RH growth**

To visualise RH growth and nucleus dynamics, we developed a CMD chip to track and image them in real time under confocal microscopy. The devices were made up of polydimethylsiloxane (PDMS), an elastomer which was covalently bound to a microscope glass coverslip. Each chip was bearing 3 independent devices, allowing one to grow three individual *Arabidopsis* seedlings in independent main channels under constant flow of  $\frac{1}{2}$  MS liquid media supplemented with sucrose (see Material and Methods). The seedlings were added into the chip prefilled with the media. To avoid crossed contamination between the channels, three independent input and output ports were used. Plantlets were germinated on  $\frac{1}{2}$

MS agar media in tips that were transferred to PDMS chip at 1 cm from the media input point and with a 45-degree angle with respect to the device (Figures 1a-b, S1a). Each device was made of 3 parallel 1.5 cm-long channels connected *via* two arrays of lateral 400  $\mu\text{m}$ -long perpendicular channels (Figures 1b, S1b). The main central channel is used for root growth, the two lateral channels for media supply, and small connecting channels for RH growth. The total volume of the chamber was 6  $\mu\text{L}$ . The root growth was under constant flow rate (8  $\mu\text{l}/\text{min}$ ) in  $\frac{1}{2}$  MS liquid media supplemented with sucrose (See Material and Methods). The device has a 250  $\mu\text{m}$ -width and 100  $\mu\text{m}$ -depth channel for the main root growth (Massalha *et al.*, 2017) (in light and dark blue respectively on Figure 1b) and 20  $\mu\text{m}$ -width and-depth lateral channels for RH expansions (in red on Figures 1b, S1b). After 4 to 5 days, a main root of  $\sim 12$  mm length could be observed in each device (Figure 1c) and the device is functional until the main root reaches the end of the main channel, which is about 8 days. Under microscope, the device was under continuous flow rate of liquid media, and RH growth could be monitored under controlled conditions with high resolution. If needed, the medium can be replaced in about 30 sec using a transient flow rate of 1000  $\mu\text{l}/\text{min}$ , lateral channels being filled simultaneously all along the chip (see figure S2 and movie S1).

### **Accurate study of the RH growth dynamics using CMD**

The RH is a differentiated cell that displays a tubular structure protruding from the surface of the root trichoblast cell. It is characterized by a polarized structure and tip expansion. The rate of RH growth has been already well described in *Arabidopsis* (Dolan *et al.*, 1994). In order to validate our microfluidic system, we measured this parameter by following growing RH for 60 min using confocal microscopy (Figure 2a, movie S2). The tip position of 29 individual RH was a linear function of time indicating a constant growth speed. To evaluate the speed of growth of each individual cell, each curve has been fitted independently with a linear model. The distribution of growth speeds had a median value around  $1.5 \pm 0.3 \mu\text{m}/\text{min}$  (Figures 2b-c). This result fits perfectly with the data of Dolan et al, describing a growth rate between 1 to 2.5  $\mu\text{m}/\text{min}$  (Dolan *et al.*, 1994). Thus our microfluidic device is suitable for the growth and study of *Arabidopsis* RH cells. pSUN2:SUN2-RFP (Tamura *et al.*, 2013) and 35S:*GFP-MBD lines* (Camilleri *et al.*, 2002) in Columbia (Col-0) background. After sterilisation, seeds were transferred into 200  $\mu\text{l}$  micro pipette tips, (cut 4 mm in height from the base) already filled with 10  $\mu\text{l}$  of  $\frac{1}{2}$  Murashige and Skoog (MS) medium (SERVA Electrophoresis) containing 0.5% sucrose and 1.0% agar. After stratification at 4°C for 48 hrs in dark, seedling were grown *in vitro* on  $\frac{1}{2}$  MS in presence of 0.5 sucrose and 1.0 % agar under long day conditions

(16-h light with 70  $\mu\text{mol}/\text{m}^2$  per second of fluorescent lighting /8-h dark conditions at 23 °C for 4-5 days (Figure S1c). Afterwards, tips with growing seedlings were transferred into the microfluidic device and put in the growth chamber for 4-5 days under a constant flow rate of medium (8  $\mu\text{l}/\text{min}$ ) supplied by a pump (Fusion 200, Chemyx) connected to the device. To label cell wall, propidium iodide (PI) was used (1  $\mu\text{g}/\text{ml}$ ).

**Confocal image acquisition and analysis.** Confocal images were recorded with a Zeiss LSM 700 confocal microscope equipped with 10 x 0.3, 20x0.8 and oil 40x1.3 lens objectives. For analysis of RH growth and nuclear dynamics, the PDMS device was maintained under continuous flow of liquid media to minimize evaporation during scanning. GFP were imaged with a 488-nm excitation and 510 nm emission wave lengths, respectively. For PI, the excitation and emission wavelengths were 555 nm and 617 nm, respectively. Imaging was performed using Z-stack ranking from 1.0 to 4  $\mu\text{m}$  during time lapse ranking from 10 to 60 min. Observations were performed in multi-tracking mode using 488 and 555-nm laser excitation. The quantification analysis was performed using ImageJ software.

**Statistical analyses.** For each distribution with a number of cell  $n < 30$  an Anderson-Darling's test was performed to test the normality of the distributions. For normal distributions or distribution with a number of cell  $n \geq 30$ , a Levene's test was performed to test the equality of the variance, then a t-test was performed using the result of the Levene's test as a parameter (equal or unequal variance).

### **Acknowledgments**

This work was supported by the Centre National de la Recherche Scientifique (CNRS) and by HFSP grant 2018, RGP, 009. This study was partially supported by the labex «Who AM I ?», labex ANR-11-LABX- 0071, and the Université de Paris, Idex ANR-18- IDEX-0001 funded by the French Government through its «Investments for the Future» program. This work was partially supported by the Inerdisciplinary Thematic Institute "IMCBio" (to M.R.), as part of the ITI 2021-2028 program of the University of Strasbourg, CNRS and Inserm, by IdEx Unistra (ANR-10-IDEX-0002), and by SFRI-STRAT'US project and EUR IMCBio (ANR-17-EURE-0023) under the framework of the French Investments for the Future Program. It was also supported by the Centre National de la Recherche Scientifique and the Université de Strasbourg whom M.R. received support from its Initiative of Excellence (IdEx)."We thank J. Mutterer for help in confocal imaging as well K. Graumann and K. Tamura for providing SUN nuclear envelope marker lines.

**Conflicts of Interest:** The authors declare no conflict of interest.

### **Author contributions**

MEC, AA, GS designed experiments. MR, SB designed and prepared the microfluidic devices.

GS, EH did experiments; GS, MEC, DP analyzed the data; GS, DP prepared the figures  
AA, GS, DP, MEC wrote the paper.

### **Data availability statement**

All relevant data are contained within the manuscript and its supporting materials.

### **Supporting Information**

Figure S1. Details of CMD chip design

Figure S2. Kinetics of media change in the device

Figure S3. Real-time position of the nucleus from the growing RH tip

Figure S4. Instantaneous velocity of the nucleus and of the RH tip

Figure S5. Shape change analysis of growing RH nuclei in real time

Movie S1. Video showing the complete exchange of the media in the device.

Movie S2. 60 min video showing RH tip expansion inside the CMD chip

Movie S3. 26 min video showing nuclear movement in the growing RH

Movie S4. 43 min video showing the high-speed nuclear movement in the mature RH

### **References**

**Agudelo, C.G., Sanati, A., Ghanbari, M., Packirisamy, M. and Geitmann, A.** (2012) A microfluidic platform for the investigation of elongation growth in pollen tubes. *J. Micromech. Microeng.*, **22**. <http://doi:10.1088/0960-1317/22/11/115009>

**Almonacid, M., Jord, A. Al, El Hayek, S., et al.** (2019) Active fluctuations of the nuclear envelope shape the transcriptional dynamics in oocytes. *Dev. Cell*, **51**, 147-157.

### **References**

**Agudelo, C.G., Sanati, A., Ghanbari, M., Packirisamy, M. and Geitmann, A.** (2012) A microfluidic platform for the investigation of elongation growth in pollen tubes. *J. Micromech. Microeng.*, **22**. <http://doi:10.1088/0960-1317/22/11/115009>

**Almonacid, M., Jord, A. Al, El Hayek, S., et al.** (2019) Active fluctuations of the nuclear envelope shape the transcriptional dynamics in oocytes. *Dev. Cell*, **51**, 147-157.

- Aufrecht, J.A., Ryan, J.M., Hasim, S., Allison, D.P., Nebenführ, A., Doktycz, M.J. and Retterer, S.T.** (2017) Imaging the root hair morphology of *Arabidopsis* seedlings in a two-layer microfluidic platform. *J. Vis. Exp.*, **126**, <http://doi:10.3791/55971>
- Balakrishnan, S., Raju, S.R., Barua, A. and Ananthasuresh, G.K.** (2020) Predicting the tension in actin cytoskeleton from the nucleus shape. *bioRxiv*. <https://www.biorxiv.org/content/early/2020/08/29/2020.08.28.272435>
- Bouhedda, F., Cubi, R., Baudrey, S. and Ryckelynck, M.** (2021)  $\mu$ IVC-Seq: A method for ultrahigh-throughput development and functional characterization of small RNAs. *Methods Mol. Biol.*, **2300**, 203–237.
- Brechenmacher, L., Nguyen, T.H.N., Hixson, K., Libault, M., Aldrich, J., Pasa Tolic, L. and Stacey, G.** (2012) Identification of soybean proteins from a single cell type: the root hair. *Proteomics*, **12**, 3365–3373.
- Brochhausen, L., Maisch, J. and Nick, P.** (2016) Break of symmetry in regenerating tobacco protoplasts is independent of nuclear positioning. *J. Integr. Plant Biol.*, **58**, 799–812.
- Bruaene, N. Van, Joss, G. and Oostveldt, P. Van** (2004) Reorganization and *in vivo* dynamics of microtubules during *Arabidopsis* root hair development. *Plant Physiol.*, **136**, 3905–3919.
- Bruaene, N. Van, Joss, G., Thas, O. and Oostveldt, P. Van** (2003) Four-dimensional imaging and computer-assisted track analysis of nuclear migration in root hairs of *Arabidopsis thaliana*. *J. Microsc.*, **211**, 167–178.
- Busch, W., Moore, B.T., Martsberger, B., et al.** (2012) A microfluidic device and computational platform for high-throughput live imaging of gene expression. *Nat. Methods*, **9**, 1101–1106.
- Camilleri, C., Azimzadeh, J., Pastuglia, M., Bellini, C., Grandjean, O. and Bouchez, D.** (2002) The *Arabidopsis* *TONNEAU2* gene encodes a putative novel protein phosphatase 2A regulatory subunit essential for the control of the cortical cytoskeleton. *Plant Cell*, **14**, 833–845.
- Chu, F.Y., Haley, S.C. and Zidovska, A.** (2017) On the origin of shape fluctuations of the cell nucleus. *Proc. Natl. Acad. Sci. USA*, **114**, 10338–10343.
- Chytilova, E., Macas, J., Sliwinska, E., Rafelski, S.M., Lambert, G.M. and Galbraith, D.W.** (2000) Nuclear dynamics in *Arabidopsis thaliana*. *Mol. Biol. Cell*, **11**, 2733–2741.

- Dolan, L., Duckett, C.M., Grierson, C., Linstead, P., Schneider, K., Lawson, E., Dean, C., Poethig, S. and Roberts, K.** (1994) Clonal relationships and cell patterning in the root epidermis of *Arabidopsis*. *Development*, **120**, 2465–2474.
- Dorland, Y.L., Cornelissen, A.S., Kuijk, C., Tol, S., Hoogenboezem, M., Buul, J.D. van, Nolte, M.A., Voermans, C. and Huveneers, S.** (2019) Nuclear shape, protrusive behaviour and in vivo retention of human bone marrow mesenchymal stromal cells is controlled by Lamin-A/C expression. *Sci. Rep.*, **9**, 1-15.
- Fal, K., Korsbo, N., Alonso-Serra, J., Teles, J., Liu, M., Refahi, Y., Chabouté, M.E., Jönsson, H. and Hamant, O.** (2021) Tissue folding at the organ-meristem boundary results in nuclear compression and chromatin compaction. *Proc. Natl. Acad. Sci. USA*, **118**. [http:// doi:10.1073/pnas.2017859118](http://doi:10.1073/pnas.2017859118)
- Fendrych, M., Akhmanova, M., Merrin, J., Glanc, M., Hagihara, S., Takahashi, K., Uchida, N., Torii, K.U. and Friml, J.** (2018) Rapid and reversible root growth inhibition by TIR1 auxin signalling. *Nat. Plants*, **4**, 453-459.
- Goswami, R., Asnacios, A., Hamant, O. and Chabouté, M.E.** (2020a) Is the plant nucleus a mechanical rheostat? *Curr. Opin. Plant Biol.*, **57**, 155–163.
- Goswami, R., Asnacios, A., Milani, P., Graindorge, S., Houlné, G., Mutterer, J., Hamant, O. and Chabouté, M.E.** (2020b) Mechanical shielding in plant nuclei. *Curr. Biol.*, **30**, 2013-2025.
- Goto, C., Tamura, K., Nishimaki, S., Maruyama, D. and Hara-Nishimura, I.** (2020) The nuclear envelope protein KAKU4 determines the migration order of the vegetative nucleus and sperm cells in pollen tubes. *J. Exp. Bot.*, **71**, 6273-6281.
- Graumann, K., Runions, J. and Evans, D.E.** (2010) Characterization of SUN-domain proteins at the higher plant nuclear envelope. *Plant J.*, **61**, 134-144.
- Grierson, C., Nielsen, E., Ketelaarc, T. and Schiefelbein, J.** (2014) Root Hairs. *The Arabidopsis Book*, American Society of Plant Biologists, **12** pp. 1-25. doi: 10.1199/tab.0172.
- Griffis, A.H.N., Groves, N.R., Zhou, X. and Meier, I.** (2014) Nuclei in motion: Movement and positioning of plant nuclei in development, signaling, symbiosis, and disease. *Front. Plant Sci.*, **5**, 1-7
- Guichard, M., Bertran Garcia de Olalla, E., Stanley, C.E. and Grossmann, G.** (2020) Microfluidic systems for plant root imaging. *Methods Cell Biol.*, **160**, 381–404.
- Hepler, P.K., Vidali, L. and Cheung, A.Y.** (2001) Polarized cell growth in higher plants. *Annu. Rev. Cell Dev. Biol.*, **17**, 159–187.

- Jiang, S., Armaly, A. and McMillan, C.** (2017) Automatically generating commit messages from diffs using neural machine translation. In *2017 32nd IEEE/ACM International Conference on Automated Software Engineering (ASE)*. pp. 135–146.
- Jones, M.A., Shen, J.-J., Fu, Y., Li, H., Yang, Z. and Grierson, C.S.** (2002) The *Arabidopsis* Rop2 GTPase is a positive regulator of both root hair initiation and tip growth. *Plant Cell*, **14**, 763–776.
- Kang, E., Zheng, M., Zhang, Y., Yuan, M., Yalovsky, S., Zhu, L. and Fu, Y.** (2017) The microtubule-associated protein MAP18 affects ROP2 GTPase activity during root hair growth. *Plant Physiol.*, **174**, 202-222.
- Ketelaar, T., Faivre-Moskalenko, C., Esseling, J.J., Ruijter, N.C.A. De, Grierson, C.S., Dogterom, M. and Emons, A.M.C.** (2002) Positioning of nuclei in *Arabidopsis* root hairs: An actin-regulated process of tip growth. *Plant Cell*, **14**, 2941-2955.
- Krupinski, P., Bozorg, B., Larsson, A., Pietra, S., Grebe, M. and Jönsson, H.** (2016) A model analysis of mechanisms for radial microtubular patterns at root hair initiation sites. *Front. Plant Sci.*, **7**. <http://doi:10.3389/fpls.2016.01560>
- Lan, P., Li, W., Lin, W.D., Santi, S. and Schmidt, W.** (2013) Mapping gene activity of *Arabidopsis* root hairs. *Genome Biol.*, **14**, R67, 1-20.
- Landrein, B., Kiss, A., Sassi, M., et al.** (2015) Mechanical stress contributes to the expression of the STM homeobox gene in *Arabidopsis* shoot meristems. *Elife*, **4**, e07811.
- Li, W. and Lan, P.** (2015) Re-analysis of RNA-seq transcriptome data reveals new aspects of gene activity in *Arabidopsis* root hairs. *Front. Plant Sci.*, **6**, 421.
- Libault, M., Farmer, A., Brechenmacher, L., et al.** (2010) Complete transcriptome of the soybean root hair cell, a single-cell model, and its alteration in response to *Bradyrhizobium japonicum* infection. *Plant Physiol.*, **152**, 541-552.
- Lockhart J.A.** (1965) An analysis of irreversible plant cell elongation. *J Theor Biol.* **8**:264-275.
- Massalha, H., Korenblum, E., Malitsky, S., Shapiro, O.H. and Aharoni, A.** (2017) Live imaging of root-bacteria interactions in a microfluidics setup. *Proc. Natl. Acad. Sci. USA*, **114**, 4549-4554.
- Meier, I., Griffis, A.H., Groves, N.R. and Wagner, A.** (2016) Regulation of nuclear shape and size in plants. *Curr. Opin. Cell Biol.*, **40**, 114–123.

- Misra, C.S., Santos, M.R., Rafael-Fernandes, M., Martins, N.P., Monteiro, M. and Becker, J.D.** (2019) Transcriptomics of *Arabidopsis* sperm cells at single-cell resolution. *Plant Reprod.*, **32**, 29-38.
- Newman-Griffis, A.H., Cerro, P. del, Charpentier, M. and Meier, I.** (2019) *Medicago* LINC complexes function in nuclear morphology, nuclear movement, and root nodule symbiosis. *Plant Physiol.*, **179**, 491–506.
- Parashar, A. and Pandey, S.** (2011) Plant-in-chip: Microfluidic system for studying root growth and pathogenic interactions in *Arabidopsis*. *Appl. Phys. Lett.*, **98**, 263703. <https://doi.org/10.1063/1.3604788>.
- Petricka, J.J., Schauer, M.A., Megraw, M., et al.** (2012) The protein expression landscape of the *Arabidopsis* root. *Proc. Natl. Acad. Sci. USA*, **109**, 6811–6818.
- Qiao, Z., Pingault, L., Zogli, P., Langevin, M., Rech, N., Farmer, A. and Libault, M.** (2017) A comparative genomic and transcriptomic analysis at the level of isolated root hair cells reveals new conserved root hair regulatory elements. *Plant Mol. Biol.*, **94**, 641-655.
- Ryu, K.H., Huang, L., Kang, H.M. and Schiefelbein, J.** (2019) Single-cell RNA sequencing resolves molecular relationships among individual plant cells. *Plant Physiol.*, **179**, 1444-1456.
- Satterlee, J.W., Strable, J. and Scanlon, M.J.** (2021) Plant stem-cell organization and differentiation at single-cell resolution. *Proc. Natl. Acad. Sci. USA*, **117**, 33689-33699.
- Shibata, M., Breuer, C., Kawamura, A., et al.** (2018) *GTL1* and *DF1* regulate root hair growth through transcriptional repression of ROOT HAIR DEFECTIVE 6-LIKE 4 in *Arabidopsis*. *Development*, **45**. <http://doi:10.1242/dev.159707>
- Sieberer, B.J., Ketelaar, T., Esseling, J.J. and Emons, A.M.C.** (2005) Microtubules guide root hair tip growth. *New Phytol.*, **167**, 711–719.
- Stanley, C.E., Shrivastava, J., Brugman, R., Heinzemann, E., Swaay, D. van and Grossmann, G.** (2018) Dual-flow-RootChip reveals local adaptations of roots towards environmental asymmetry at the physiological and genetic levels. *New Phytol.*, **217**, 1357-1369.
- Sun, L., Liu, L., Lin, X., Xia, Z., Cao, J., Xu, S., Gu, H., Yang, H. and Bao, N.** (2021) Microfluidic devices for monitoring the root morphology of *Arabidopsis thaliana* in situ. *Anal. Sci. Int. J. Japan Soc. Anal. Chem.*, **37**, 605–611.
- Tamura, K., Iwabuchi, K., Fukao, Y., Kondo, M., Okamoto, K., Ueda, H., Nishimura, M. and Hara-Nishimura, I.** (2013) Myosin XI-i links the nuclear membrane to the

- cytoskeleton to control nuclear movement and shape in arabidopsis. *Curr. Biol.*, **23**, 1776-1781.
- Vassileva, V.N., Kouchi, H. and Ridge, R.W.** (2005) Microtubule dynamics in living root hairs: transient slowing by lipochitin oligosaccharide nodulation signals. *Plant Cell*, **17**, 1777–1787.
- Versaevel, M., Grevesse, T. and Gabriele, S.** (2012) Spatial coordination between cell and nuclear shape within micropatterned endothelial cells. *Nat. Commun.*, **14**, 1-11.
- Volgger, M., Lang, I., Ovecka, M. and Lichtscheidl, I.** (2010) Plasmolysis and cell wall deposition in wheat root hairs under osmotic stress. *Protoplasma*, **243**, 51–62.
- Wymer, C.L., Bibikova, T.N. and Gilroy, S.** (1997) Cytoplasmic free calcium distributions during the development of root hairs of *Arabidopsis thaliana*. *Plant J.*, **12**, 427-439.
- Yamada, M. and Goshima, G.** (2018) The KCH kinesin drives nuclear transport and cytoskeletal coalescence to promote tip cell growth in *Physcomitrella patens*. *Plant Cell*, **30**, 1496–1510.
- Yi, K., Menand, B., Bell, E. and Dolan, L.** (2010) A basic helix-loop-helix transcription factor controls cell growth and size in root hairs. *Nat. Genet.*, **42**, 264–267.
- Zhang, S., Liu, J., Xue, X., Tan, kang, Wang, chunbo and Su, H.** (2019) The migration direction of hair cell nuclei is closely related to the perinuclear actin filaments in *Arabidopsis*. *Biochem. Biophys. Res. Commun.*, **519**, 783-789.

### Figure Legends:

**Figure 1.** Experimental procedure and CMD chip details for RH analysis. (a) Top view of 9 days old *Arabidopsis* seedlings growing in a micro pipette tip, filled with ½ MS media. Tips were inserted in CMD chip. (b) A schematic 3D diagram of the CMD design with the illustration of root and RH in main and side channels, respectively. Light blue colour indicates widths of the main channel and length of the lateral channels. The depths of the main and lateral channels are indicated in blue and red, respectively. (c) A 10x magnification image of root grown in the CMD with RH expanding in the lateral channels. Plantlets expressing the nuclear envelope marker SUN1-GFP were used here, and fluorescence images highlighting the root, RH and nuclei were merged with DIC visualization of the PDMS chip (Scale bar: 100µm).

**Figure 2.** *Arabidopsis* RH tip growth in real time. (a) Bright field sequential images from a time-lapse recording of *Arabidopsis* growing RH to follow the tip growth. Pictures were taken every min (Movie S2) but presented here with only 10 min intervals. (b) Growth curves of individual RH (n=29). (c) The distribution of the average speeds of the growing RH has a median of 1.5  $\mu\text{m}/\text{min}$  (. Live imaging was recorded using 10x magnification (n = 29, scale bar: 20  $\mu\text{m}$ ).

**Figure 3.** Nuclear migration in growing RH of an *Arabidopsis* line expressing the SUN2-RFP nuclear envelope marker. (a) Nucleus (in red) maintains a fixed position compared to the RH tip (in grey). Time lapse over 16 min and Z stack (1 $\mu\text{m}$ -21 slides) recording of 2 RH presented here as sum slices projection over 2 min intervals. Brown and yellow lines : lines over which were determined the positions of the nuclei and RH tip over time for, for cell 1 and cell 2 respectively. These positions were used to get the kymographs of Figure 3b, and curves of Figures 3c and 3d indicate the trajectories followed by the nuclei 1 and 2 in their respective cells (b) Kymographical representation of RH tip (top) and nuclear (bottom) positions in a growing RH (cell 1). (c-d) A graphical representation of nuclear (red) and tip position (blue) during RH growth. The distance between nucleus and RH tip was evaluated (yellow). Circles and triangles are for cell1 and cell 2, respectively. Scale bar 20  $\mu\text{m}$ .

**Figure 4.** *In vivo* time-laps imaging to show fluctuations in the nuclear shape of growing RH in real time. (a) 10 min sequence of time laps recording of *SUN1-GFP* RH nucleus. Z stacked images are presented (sum slices projection). Pictures were taken every min (Movie S4). (b) Analysis of nuclear shape fluctuation in real time by presenting aspect ratio, nuclear area, perimeter and circularity. These 2D parameters were determined in a typical interval of 5% of the measured value. (scale bar: 10  $\mu\text{m}$ ). Measurements for other RH nuclei are presented in Figure S5. (c) Focus on 3D shape changes. The left column displays the 2D section of the nucleus undergoing the most important shape change over 2 minutes. the 3 remaining columns display 3D reconstructions of the nucleus in different views. PI staining (in red) reveals the RH cell wall. (d) Transverse section view (Y-Z plane) showing the nuclear shape changes over time. (e) Nuclear volume as function of time. Nuclear volumes estimated from z-stacks were determined in a typical interval of 20% of the measured value (scale bar: 5  $\mu\text{m}$ ).

**Figure 5.** Comparison of the positions and shapes of growing and mature RH nuclei. (a) Representative images of the position of the nucleus during the growing and mature phases

(PI in red, SUN1-GFP in green, scale bar: 20  $\mu\text{m}$ ). (b) Quantification of the distance between the nucleus and the tip for growing and mature RH cells (n=23) (c-d) Quantification of the nuclear projected area (c) and the nucleus aspect ratio (d) of growing (n=38) and mature (n=35) RH. t-test; \*\*\*\* $p < 0.0001$

### Supplemental Figure Legends

**Figure S1.** (Details of CMD chip design a-b) Detail measurement of CMD chip indicating main channels 90 degree-oriented side channels (c) 5 days old *Arabidopsis* seedlings. grown into micro pipette tip contain  $\frac{1}{2}$  MS media supplemented with 0.5% sugar and 1% agar.

**Figure S2:** Kinetics of media exchange in the device. (a) Image of the microfluidic chip filled with xylene blue. The yellow line represents the line used to do the kymograph of figure (b) below. (b) Kymograph extracted from the movie S1. Each vertical line reports the color time evolution inside a given lateral channel, and thus to what extent it is filled at a given time. After 29 seconds, one can consider that the lateral channels are fully filled with xylene blue since there is no noticeable changes in the colors below the horizontal line at 29 s. Please note that the appearance of such horizontal lines indicate that lateral channels are filled ~simultaneously all along the chip. Scale bar 400  $\mu\text{m}$ .

**Figure S3.** Real-time position of the nucleus from the growing RH tip. Nuclear distance from the growing RH tip remains more or less constant. Measurement of the nuclear distance from *pSUN2:SUN2-RFP Arabidopsis* RH tip for individual nuclei at each min. during 10 min. Confocal images were analysed with maximal Z stack projections (n=5).

**Figure S4:** Instantaneous velocity of the nucleus (yellow) and of the RH tip (black). On long time scales, the instantaneous speed of the nucleus may display fluctuations, but its values are always centred around the rate at which the RH tip is growing. This implies that the mean speeds of the nucleus and RH tip are ~equal and that, during growth, the nucleus is located at a fixed distance from the RH tip, even though displaying fluctuations around its mean position. Images were acquired every 10 min with a 20X objective.

**Figure S5:** Shape change analysis of growing RH nuclei in real time. Shape change analysis of the growing RH nuclei in real time. Measurement of change in aspect ratio. area. perimeter

and circularity of 12 individual RH nuclei. 10 minutes imaging were performed with 1 min/Z stack (n=12).

**Movie S1.** 1.46 min real-time video showing complete filling of the device with xylene blue at a 1000  $\mu\text{l}/\text{min}$  flow rate. Scale bar 400  $\mu\text{m}$ .

**Movie S2.** 60 min video. showing RH tip expansion inside the CMD chip (PI in red. scale bar=50  $\mu\text{m}$ ). 5fps video

**Movie S3.** 26 min video. showing nuclear movement in growing RH expressing the nuclear envelope marker *pSUN2::SUN2-RFP* into the CMD chip (scale bar=10  $\mu\text{m}$ ). 5fps video

**Movie S4.** 43 min video showing high speed nuclear movement inside the mature RH expressing the nuclear envelope marker *pSUN1::SUN1-GFP* (PI in red. scale bar= 10  $\mu\text{m}$ ). 5fps video

Figure 1

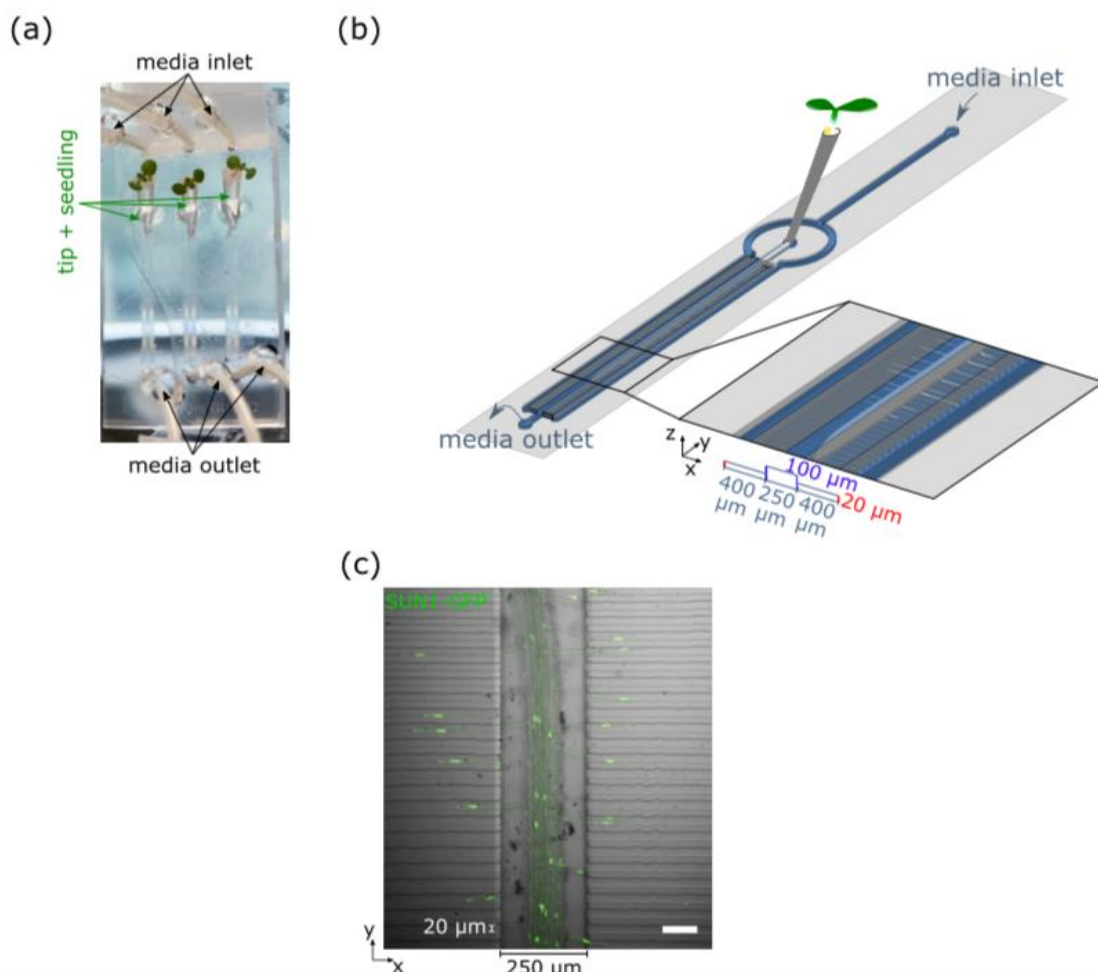


Figure 2

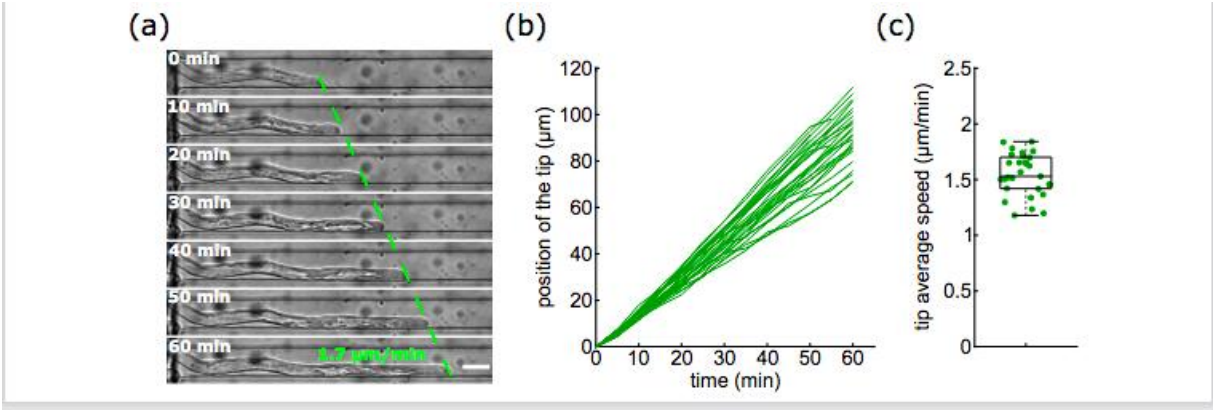


Figure 3

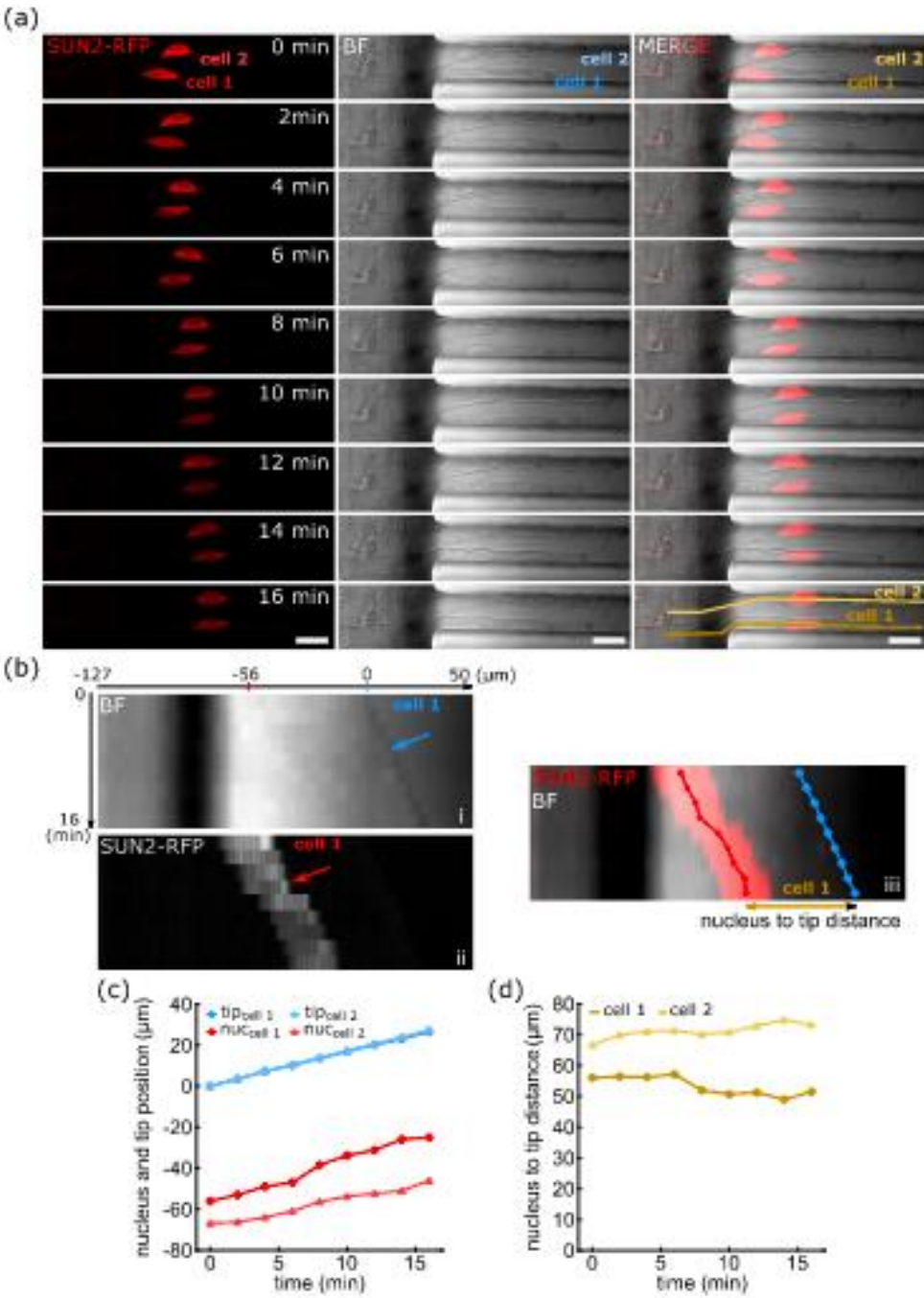


Figure 4

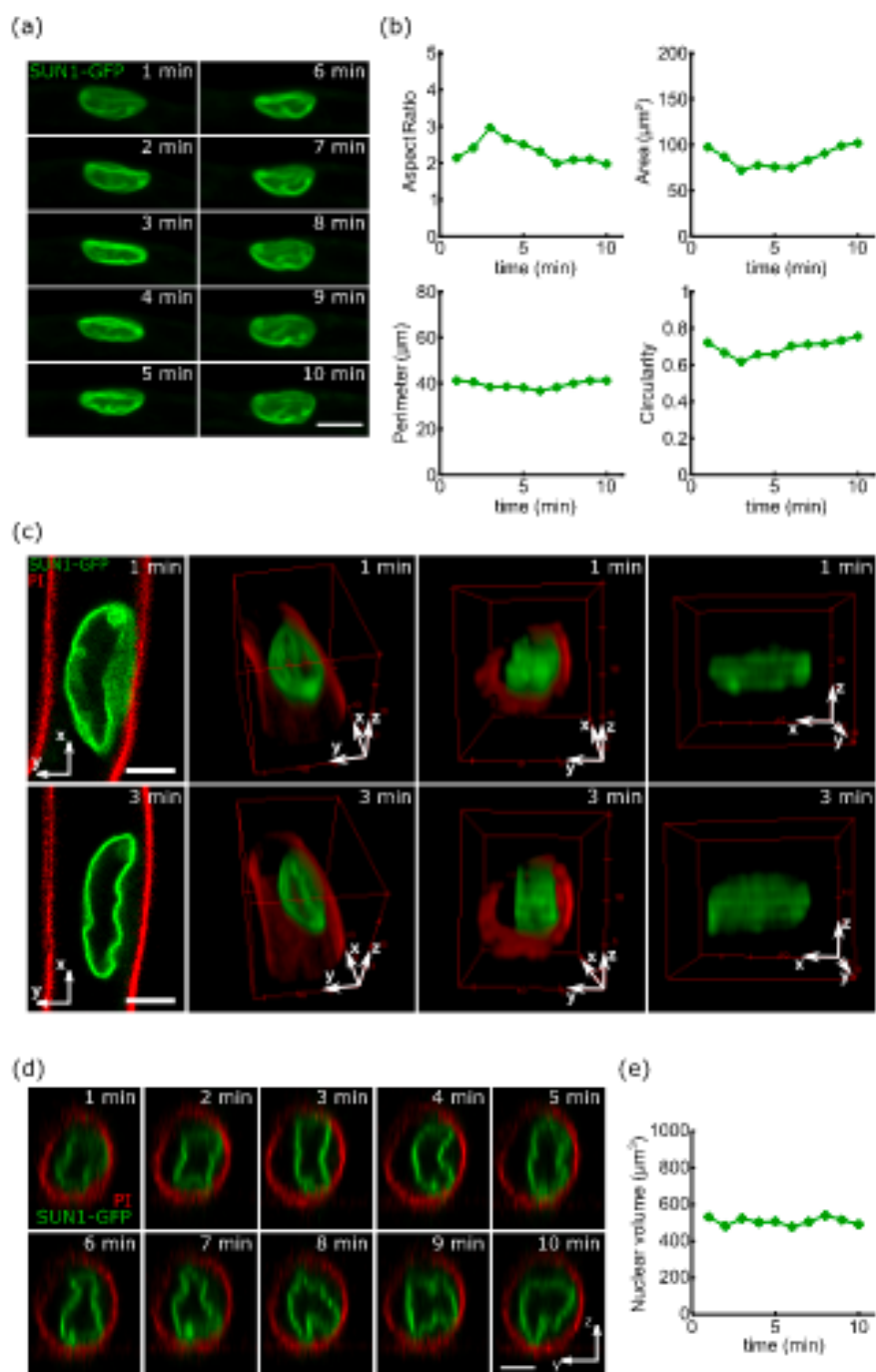
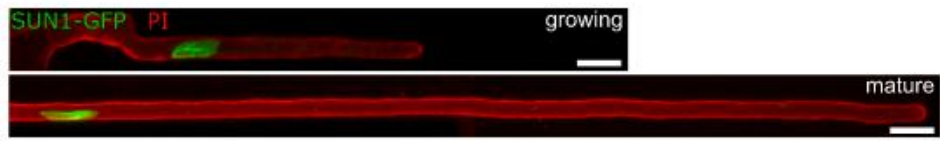
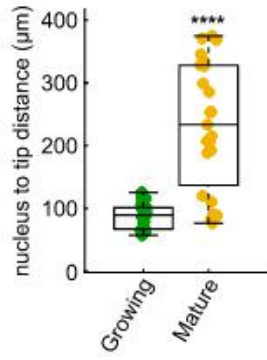


Figure 5

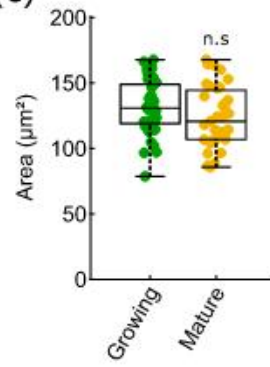
(a)



(b)



(c)



(d)

